

# Adsorption of $\text{H}_4\text{SiO}_4$ as a Hydrolysate of Sodium Silicate on Surfaces of Fluorite (111), Calcite (104), and Scheelite (112): a Density Functional Theory Approach

Yun-ye Cao<sup>1</sup>, Yue Zhang<sup>2,\*</sup>

<sup>1</sup> School of Material Science and Chemical Engineering, Ningbo University, Ningbo 315211, P.R. China;

<sup>2</sup> Department of Civil Engineering, Qingdao University of Technology, Qingdao 266033, P.R. China;

\*E-mail: [zhangyue1723@gmail.com](mailto:zhangyue1723@gmail.com)

Received: 8 August 2019 / Accepted: 10 October 2019 / Published: 29 October 2019

---

$\text{H}_4\text{SiO}_4$ , a hydrolysate of sodium silicate, is the important species in the adsorption process during flotation separation. In this work, the interaction mechanism and adsorption behavior in the surface-chemistry of  $\text{H}_4\text{SiO}_4$  molecule on the most stable surfaces of three calcium minerals, fluorite (111), calcite (104), and scheelite (112), were investigated systemically by using ab-initio calculation because the lack experimental approaches at the atomistic level. The results indicated that electrostatic interactions occurred between the electronegative oxygen atom of the  $\text{H}_4\text{SiO}_4$  molecule and a calcium atom on the mineral surfaces, hydrogen bonds was observed between the hydrogen atoms of the  $\text{H}_4\text{SiO}_4$  molecule and an oxygen atom or a fluorine atom of the calcium mineral surface, and the OH groups of  $\text{H}_4\text{SiO}_4$  were significantly stretched during adsorption. The adsorption energy of  $\text{H}_4\text{SiO}_4$  molecule on the surfaces of fluorite (111), calcite (104), and scheelite (112) were -1.72, -1.21, -1.55 eV, respectively. Hence, fluorite and calcite were the most and the least sensitive mineral to the adsorption of  $\text{H}_4\text{SiO}_4$  during flotation separation, respectively. The electronic structure show that the chemisorption of  $\text{H}_4\text{SiO}_4$  molecules on the surfaces of calcium minerals could change electron distribution and the overlaps between Ca-3p and O-2s orbitals and Ca-3d and O-2p orbitals, which led to the formation of new O-Ca bonds.

---

**Keywords:**  $\text{H}_4\text{SiO}_4$ ; adsorption; calcium minerals; DFT

## 1. INTRODUCTION

Scheelite ( $\text{CaWO}_4$ ) is an important tungsten bearing mineral, its separation from calcium gangue minerals [1-4], such as calcite ( $\text{CaCO}_3$ ) and fluorite ( $\text{CaF}_2$ ), has attracted scientific interest [5-9]. However, its process faces a difficult problem, because [10-14] calcium minerals have a semi-soluble nature, similar surface properties, and the same active homogeneous cation ( $\text{Ca}^{2+}$ ) site [15-18] that result

in similar responses to variety of depressants which are currently using, such as sodium silicate. Depressants allows surface-chemistry-based processes in flotation separation for the inhibiting of Ca-bearing gangue minerals that make use of the differences in adsorption on the surfaces of Ca-bearing mineral. Therefore, studying the adsorption surface-chemistry between sodium silicate and the surfaces of calcium minerals is highly important in flotation separation. The solution chemistry of sodium silicate is complex [19], because its hydrolysis produces several monomeric, polymeric, and colloidal species (Sjöberg and Öhman).  $\text{H}_4\text{SiO}_4$  is the predominant species below pH 9.8 [19,20], and above which are the monosilicate ions. Thus, the function of sodium silicate depends on the concentration and flotation pH. Considering the hydrolysis of sodium silicate in the process, previous studies [2, 11, 19, 21] focused on the adsorption mechanisms of sodium silicate on surfaces of Ca-bearing mineral still cannot seek to determine how the hydrolysate of sodium silicate is adsorbing on calcium mineral surfaces, as well as the mode of adsorption at different pH values. Moreover, the interaction mechanism has not been described yet at the atomic level, because no method can directly monitor initial reactions and obtain in-situ kinetics data in the present study.

In such scenario, the study on the interaction mechanism of  $\text{H}_4\text{SiO}_4$  as a predominant hydrolysate of sodium silicate below pH 9.8 on different surfaces of calcium minerals faces a dilemma in terms of adsorption process. Molecular modeling [22-25] is a valuable tool for providing a fundamental information of chemical reactions at the atomic level. In this article, we have investigated the interaction mechanism of  $\text{H}_4\text{SiO}_4$  as a hydrolysate of  $\text{Na}_2\text{SiO}_3$  on different surfaces of Ca-bearing minerals and established a link between the difference of adsorption behaviors and local surface chemistry. Density Functional Theory (DFT) simulations, proved as an effective approach for studying the interaction mechanism [26-29], has revealed the adsorption configuration, adsorption site, reaction pathway, electronic structure, and adsorption energy, which could provide theoretical reference for the flotation separation of calcite, fluorite and scheelite in essence.

## 2. METHODS

The ab-initial calculations in this study were performed by using Vienna Ab-initio Simulation Package (VASP), with the projector augmented wave (PAW) method. The GGA-PBE method was chose as the exchange-correlation potential function [30]. The k-mesh of Brillouin zone [31] was generated by Monkhorst-Pack grids. We used  $3 \times 3 \times 3$  k-points for unit cell ionic geometry optimization and  $2 \times 2 \times 1$  k-points for  $\text{H}_2\text{SiO}_4$  adsorption. The k-mesh was tested previously to ensure its accuracy for all the structures in the DFT calculation. The cut-off energy was set to 500 eV, which was determined to be sufficient to obtain fully converged results.

The geometry optimization was performed by using the conjugate gradient method. The ionic relaxation would be stopped if all forces were smaller than  $0.02 \text{ eV}/\text{\AA}$ . First, the lattice parameters were calculated for fluorite, calcite and scheelite unit cell. The obtained lattice parameters a, b and c as shown in Table 1 were in good agreement the experimental measurements and previous ab-initial calculations results.

**Table 1.** Comparison of calculated and experimental lattice parameters of calcite, fluorite and scheelite unit cell

mineral	resource	a	b	c	$\alpha$	$\beta$	$\gamma$
calcite	This work	5.06	5.06	16.92	90.00	90.00	120.00
	DFT [32]	5.06	5.06	17.25	90.00	90.00	120.00
	Experimental [33]	4.99	4.99	17.06	90.00	90.00	120.00
fluorite	This work	5.52	5.52	5.52	90.00	90.00	90.00
	DFT [34]	5.46	5.46	5.46	90.00	90.00	90.00
	Experimental [35]	5.46	5.46	5.46	90.00	90.00	90.00
scheelite	This work	5.00	5.00	10.73	90.00	90.00	90.00
	DFT [36]	5.33	5.33	11.57	90.00	90.00	90.00
	Experimental [37]	5.24	5.24	11.38	90.00	90.00	90.00

Inspired by previous studies, this work chose the most stable surfaces of the three calcium-bearing minerals [10, 32, 38]. For fluorite, calcite, and scheelite, the (111), (104), and (112) crystal surfaces, respectively, were chosen for studying the adsorptions behavior of  $\text{H}_4\text{SiO}_4$  on the surfaces. It would be certainly conducive to Ca-bearing mineral floatation. The surface model for each kind of mineral was obtained by cleaving the unit cell and extend to an appropriate size. The height of the vacuum upon the slab is set to 15 Å to avoid the interaction between adjacent images. We tested different cleavage position and the thickness of the surface slab, chose the structure with the lowest energy for the adsorption calculation. In the initial configuration before the geometry optimization, a  $\text{H}_4\text{SiO}_4$  molecule was placed on a Ca-bearing mineral surface, a series of initial configuration was test to find the most stable sturcutre for  $\text{H}_4\text{SiO}_4$  adsorption.

The adsorption energy was calculated as follows [39]:

$$E_{ads} = E_{total} - E_{surface} - E_{molecule}$$

1)

where  $E_{ads}$  is the adsorption energy,  $E_{total}$  is the total energy of the  $\text{H}_4\text{SiO}_4$  – surface system,  $E_{surface}$  is the energy of the calcium mineral (fluorite (111), calcite (104) and scheelite (112)) surface, and  $E_{molecule}$  was the energy of the free  $\text{H}_4\text{SiO}_4$  molecule. A negative adsorption energy calculated in this equation indicates an exothermic reaction and a lower adsorption energy means a stronger interaction between adsorbate and mineral surface.

### 3. RESULTS AND DISCUSSION

#### 3.1 Adsorption of $H_4SiO_4$ on fluorite (111) surface

The adsorption of a  $H_4SiO_4$  molecule on fluorite (111) surface was calculated, the most stable structure was obtained after geometry optimization. In this structure, the  $H_4SiO_4$  molecule adsorbed on the fluorite (111) surface molecularly, as shown in Figure 1.

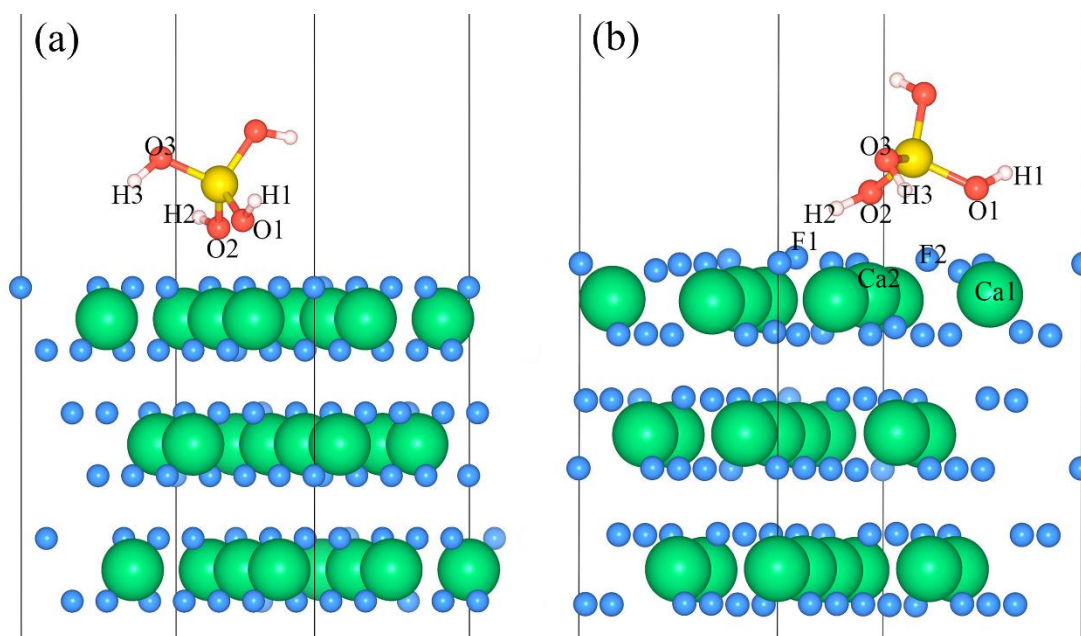


**Figure 1.** Top views of a  $H_4SiO_4$  molecule adsorbing on the fluorite (111) surface: (a) initial structure; (b) final structure after geometric optimization. Color scheme: green, blue, yellow, red, and white represented Ca, F, Si, O, and H atoms, respectively.

It can be gotten from Fig. 1 two Ca-O bonds formed between the oxygen atom of  $H_4SiO_4$  molecule and the Ca atom of on the topmost surface. The bond length of two Ca-O bond are 2.56 and 2.66 Å, respectively. Moreover, the OH group of the  $H_4SiO_4$  molecule tilts toward the adjacent F atom, forming a hydrogen bond between the H atom of  $H_4SiO_4$  molecule and F atom of fluorite (111) surface with F-H bond distances of 1.57 and 1.76 Å, respectively. These two OH bond lengths of  $H_4SiO_4$  were stretched from 0.97 and 0.97 Å to 1.01 and 0.99 Å, respectively, which indicated a negligible distortion of  $H_4SiO_4$ . The adsorption energy of this process was -1.72 eV, which was the highest among the three calcium minerals, and indicated that  $H_4SiO_4$  was preferentially adsorbing on a fluorite (111) surface.

**Table 2.** Adsorption energy and geometric properties of the adsorption system of a  $H_4SiO_4$  molecule on fluorite (111), calcite (104), and scheelite (112) surface

mineral	Ca1-O1	Ca2-O2	F2-H2	F3-H3	O2-H2	O3-H3	O <sub>c</sub> 2-H2	O <sub>c</sub> 3-H3	E <sub>ads</sub> (ev)
fluorite	2.56	2.66	1.57	1.76	1.01	0.99			-1.72

calcite	2.62	2.55	-	-	1.05	1	1.48	1.72	-1.21
scheelite	2.48	2.45	-	-		0.99		1.76	-1.55
H <sub>4</sub> SiO <sub>4</sub>					0.97	0.97			

Note: As mentioned Ca1-O1 and Ca2-O2, Ca1 and Ca2 belong to the calcium mineral molecule, and O1 and O2 belong to the H<sub>4</sub>SiO<sub>4</sub> molecule; For F2-H2 and F3-H3, F2 and F3 belong to the fluorite molecule, and H2 and H3 belong to the H<sub>4</sub>SiO<sub>4</sub> molecule; For O2-H2, O3-H3, Oc2-H2, and Oc3-H3, Oc2 and Oc3 belong to the calcite or scheelite molecule, and O2, O3, H2, and H3 belong to the H<sub>4</sub>SiO<sub>4</sub> molecule.

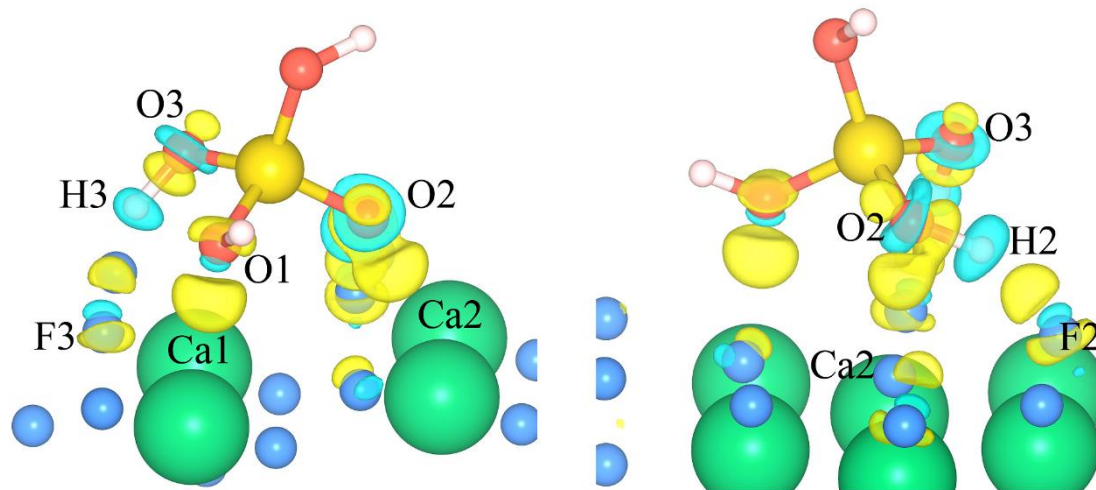


**Figure 2.** Charge density difference of the most stable adsorption configuration of H<sub>4</sub>SiO<sub>4</sub> molecule on fluorite (111) surface. An isosurface with a charge density of 0.003 e/Å<sup>3</sup> is used, where charge depletion and accumulation were indicated in light greenish-blue and bright yellow, respectively. Color scheme: green, blue, yellow, red, and white represented Ca, F, Si, O, and H atoms.

The calculated energy of adsorption and geometric properties for the adsorption of a H<sub>4</sub>SiO<sub>4</sub> molecule on fluorite, calcite and scheelite surfaces were shown in Table 2. The charge density difference of the adsorption system of the H<sub>4</sub>SiO<sub>4</sub>-fluorite (111) surface was illustrated in Figure 2. The Bader charge of the adsorbate and surface showed that the H<sub>4</sub>SiO<sub>4</sub> molecule accepted electrons from the fluorite (111) surface during adsorption. The negative charge on the F2, and F3 atoms that bonded with the H atoms of H<sub>4</sub>SiO<sub>4</sub> molecule by hydrogen bond, decreased by 0.02 e<sup>-</sup> and 0.03 e<sup>-</sup> respectively. The positive charge on the corresponding hydrogen atoms decreased by 0.02 e<sup>-</sup> and 0.04 e<sup>-</sup> respectively, whereas the negative charges on O1, O2 and O3 atoms increased by 0.02 e<sup>-</sup>, 0.06 e<sup>-</sup> and 0.06 e<sup>-</sup>, respectively. This remarkable increase of O charge mainly contributed to electron density reduction of the adjacent calcium atoms. The Bader charges of the Ca1, Ca2 and Ca3 atoms increased by 0.02, 0.03 and 0.04 e<sup>-</sup>, respectively, indicating O atoms in H<sub>4</sub>SiO<sub>4</sub> molecule were adsorbing the surface Ca atoms.

The partial density of states (PDOS) of H<sub>4</sub>SiO<sub>4</sub>-fluorite (111) system was calculated to characterize the bond formation mechanism in the adsorption process.

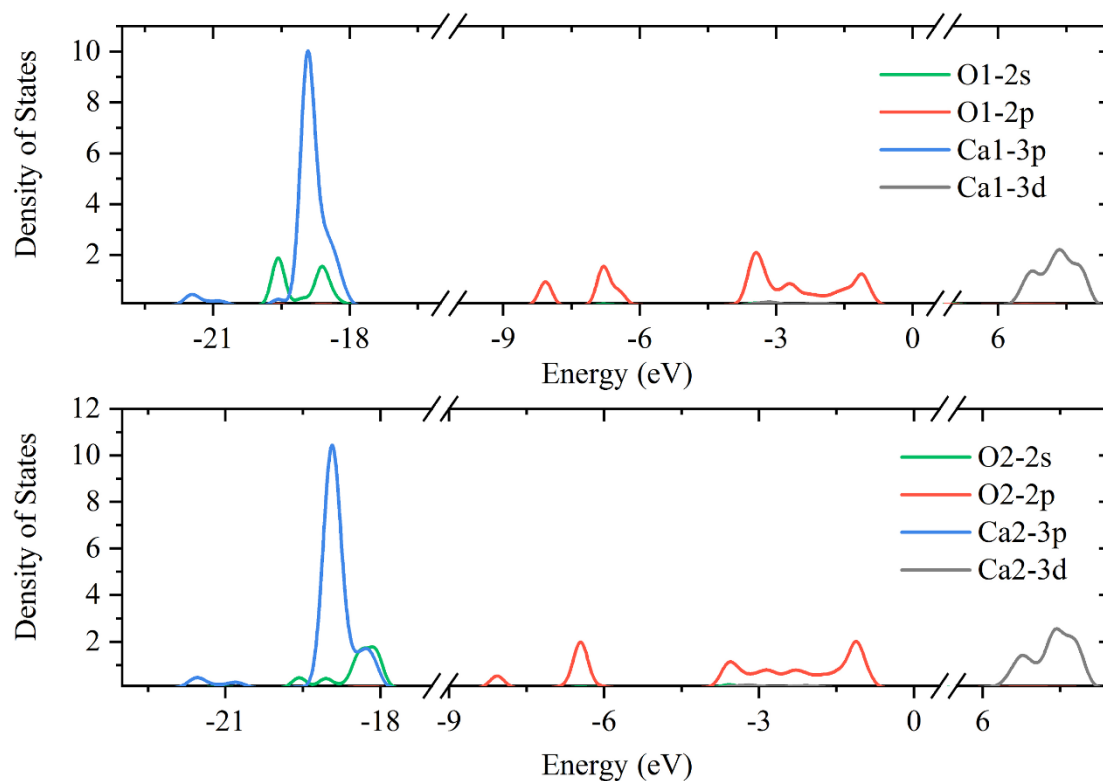


**Figure 3.** PDOS of the adsorption surface of the  $\text{H}_4\text{SiO}_4$ -fluorite (111) system. The calculated Fermi level is set as the zero point of x-axis. The curves correspond to the PDOS projected on to O atoms of  $\text{H}_4\text{SiO}_4$  and the two adjacent Ca atoms. Ca1, and Ca2 are labeled Figure 2.

The partial density of states (PDOS) of the  $\text{H}_4\text{SiO}_4$ -fluorite (111) system was calculated as shown in Fig. 3. The PDOS shows a significant overlaps between the O1-2s and Ca1-3p orbital in the range of -19.30 eV to -17.97 eV, and between O2-2p and Ca2-3d orbital from -3.69 eV to -1.72 eV. These overlaps leads the formations of Ca-O chemical bonds between the oxygen atoms of  $\text{H}_4\text{SiO}_4$  and Ca atoms of fluorite (111) surface.

### 3.2 Adsorption of $\text{H}_4\text{SiO}_4$ on calcite (104) surface

Adsorption of a  $\text{H}_4\text{SiO}_4$  molecule on the surface of calcite (104) was calculated. Molecule was initially placed above calcium atoms of the calcite (104) surface the most stable structure, adsorption energy and surface reconstruction are obtained, as shown in Figure 4.

In the most stable structure of calcite (104) surface, two Ca-O bonds are found between the oxygen atom of  $\text{H}_4\text{SiO}_4$  molecule and the calcium atom of calcite surface with the bond length of 2.55 and 2.62 Å. The OH group of  $\text{H}_4\text{SiO}_4$  molecule tilts toward the adjacent O atom, a H-bond was found between the hydrogen atom of  $\text{H}_4\text{SiO}_4$  and the oxygen atom of calcite surface. The formed H-bond length was calculated as 1.48 and 1.72 Å, respectively. On the other hand, the O-H bond length in  $\text{H}_4\text{SiO}_4$  molecule were stretched from 0.97 and 0.97 Å to 1.05 and 1.00 Å, which indicates a slight distortion of  $\text{H}_4\text{SiO}_4$  molecule in the adsorption process. The adsorption energy of  $\text{H}_4\text{SiO}_4$  on calcite (104) surface is -1.21 eV, which is the lowest in the adsorption system of  $\text{H}_4\text{SiO}_4$  among the three calcium minerals

investigated in this research. It indicates that calcite is the least sensitive mineral to adsorption of  $\text{H}_4\text{SiO}_4$  in the flotation process.

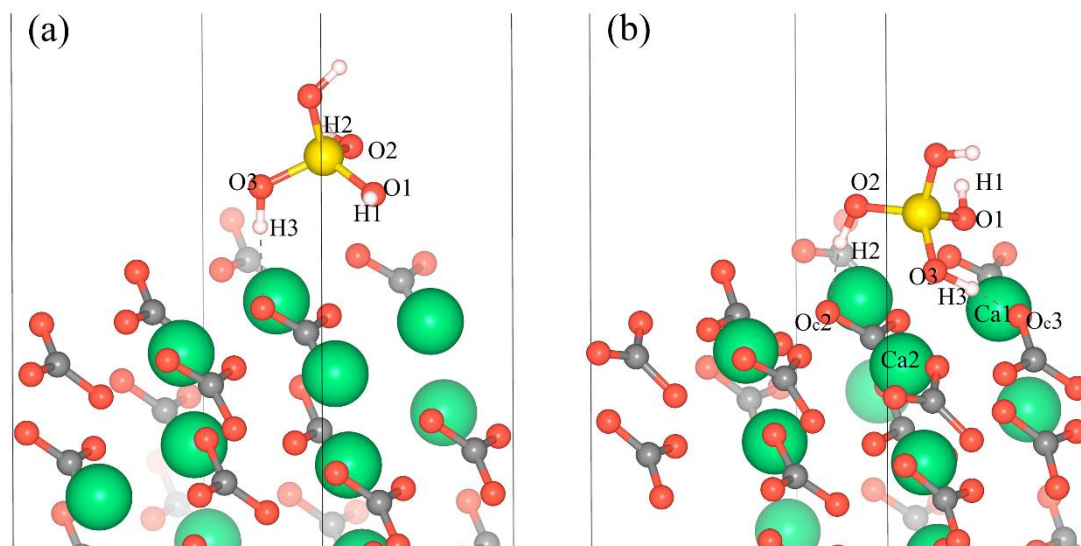


**Figure 4.** Side views of a  $\text{H}_4\text{SiO}_4$  molecule adsorbing on a calcite (104) surface: (a) initial structure, (b) final structure after geometric optimization. Color scheme: red, green, gray, white, and yellow represented O, Ca, C, H and Si atoms.

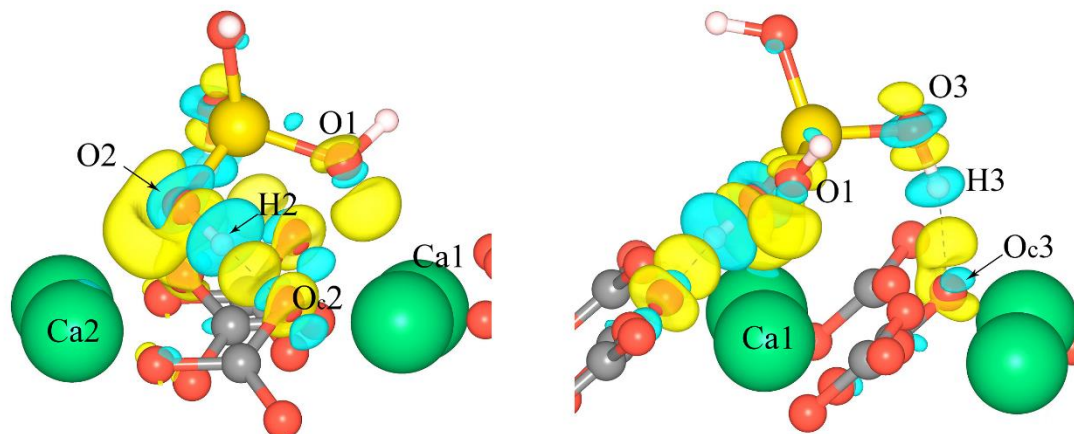


**Figure 5.** Charge density difference of the most stable adsorption configuration of a  $\text{H}_4\text{SiO}_4$  molecule on a calcite (104) surface. An isosurface of charge density of  $0.003 \text{ e}^-/\text{\AA}^3$  is used, where charge depletion and accumulation were indicated in light greenish-blue and bright yellow, respectively. Color scheme: red, green, gray, yellow, and white represent O, Ca, C, Si and H atoms.

The charge density difference of the adsorption system was illustrated in Figure 5. Bader charge calculation indicates that the  $\text{H}_4\text{SiO}_4$  molecule behaved as an electron acceptor while calcite (104) surface was the electron donor in the adsorption process. The negative charge on the  $\text{O}_{\text{e}2}$ ,  $\text{O}_{\text{e}3}$  atoms bonded with H atoms of  $\text{H}_4\text{SiO}_4$  molecule by hydrogen bond, decreased by  $0.02 \text{ e}^-$  and  $0.01 \text{ e}^-$ . The positive charge on the corresponding hydrogen atoms decreased by  $0.04 \text{ e}^-$  and  $0.02 \text{ e}^-$ , whereas the

negative charges on O2 and O3 atoms increased by  $0.08 e^-$  and  $0.04 e^-$ . The significant increases in the O atom charge was because of reduction of the electron density of the bonded calcium atoms. The bader charges of the Ca1 and Ca2 atoms increased by  $0.01$  and  $0.02 e^-$ , respectively. It indicates that O atoms of  $H_4SiO_4$  molecule were adsorbing the surface Ca atoms during adsorption.

The partial density of states (PDOS) of  $H_4SiO_4$ -calcite (104) system was calculated to characterize the bond formation mechanism in the adsorption process, as shown in Fig.6.

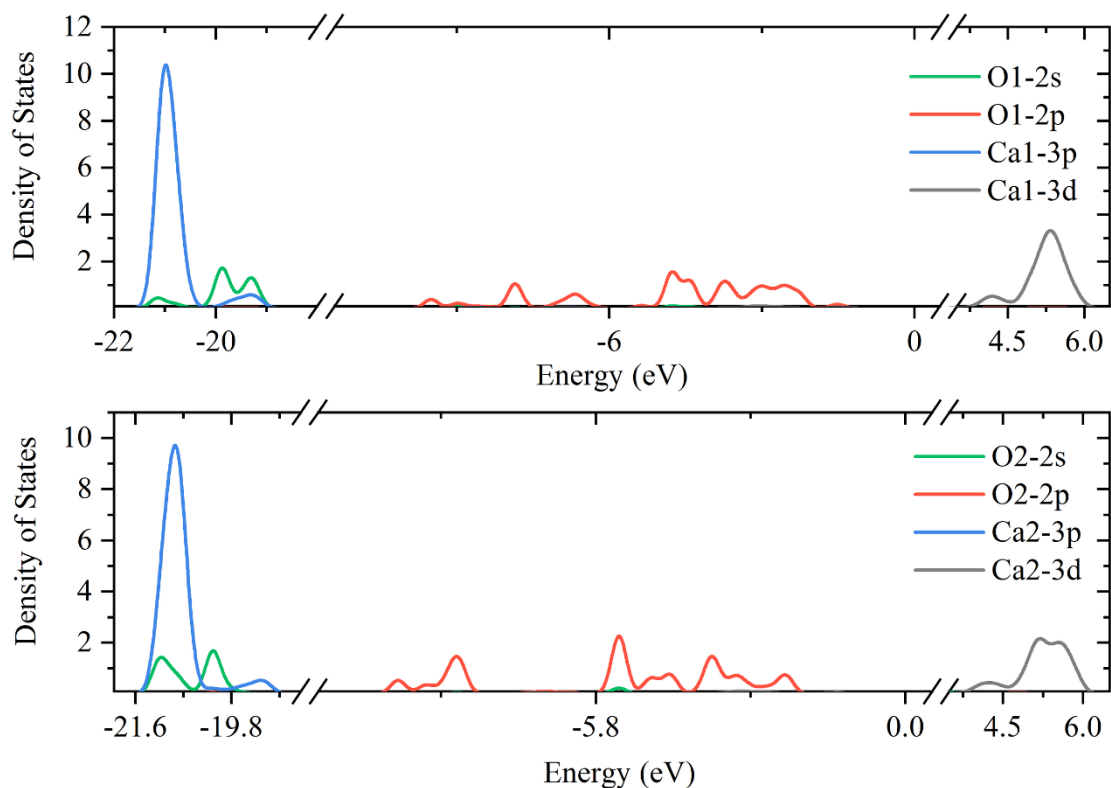


**Figure 6.** PDOS of the adsorption surface of the  $H_4SiO_4$ -calcite (104) system. The calculated Fermi level is set as the zero point of x-axis. The curves represent the PDOS projected on to the two adjacent Ca atoms and O atoms of  $H_4SiO_4$ . Ca1, and Ca2 are labeled in Figure 5.

The obtained PDOS of the surface atoms and adsorbed  $H_4SiO_4$  molecule were plotted in Figure 6. Results shows that there were significant overlaps between the O1-2s and Ca1-3p orbital's from -21.43 eV to -18.94 eV, and O2-2p and Ca2-3d orbital in the range of -3.57 eV to -2.28 eV. The overlapping of electronic orbital caused the formation of Ca-O chemical bonds between the O atom of  $H_4SiO_4$  and the Ca atoms of calcite (104) surface, which is similar as when  $H_4SiO_4$  absorbed the mineral surface (Fig. 3).

### 3.3 Adsorption of $H_4SiO_4$ on scheelite (112) surface

$H_4SiO_4$  molecule was initially placed above calcium atoms of the scheelite (112) surface, the most stable structure, adsorption energy and surface reconstruction are obtained, as shown in Figure 4.

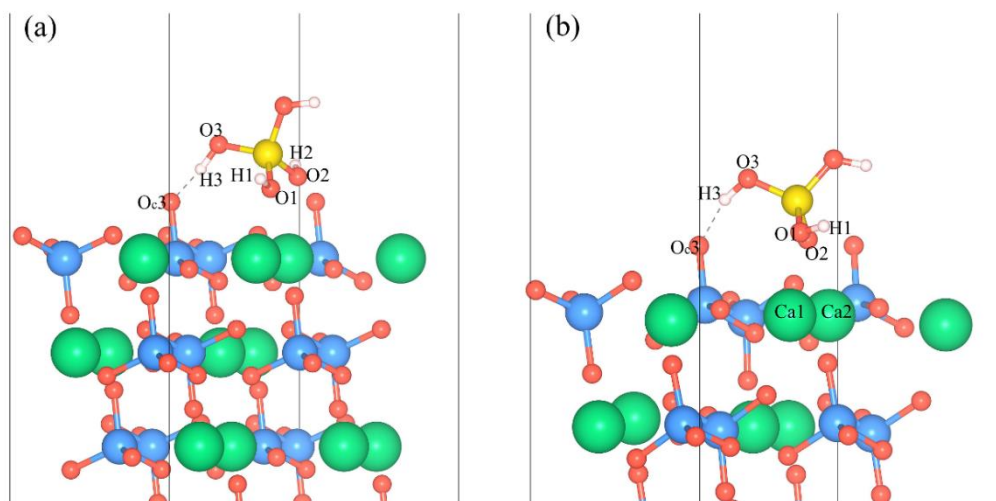


**Figure 7.** Side views of a  $\text{H}_4\text{SiO}_4$  molecule adsorbing on the scheelite (112) surface: (a) initial structure, (b) final structure after geometric optimization. Color scheme: green, blue, red, white, and yellow represented Ca, W, O, H and Si atoms.

In the most stable structure of scheelite (112) surface, two Ca-O bonds were found between the O atoms of  $\text{H}_4\text{SiO}_4$  molecule and the surface of Ca atoms with bond lengths of 2.62 and 2.55 Å. The adsorption system of  $\text{H}_4\text{SiO}_4$  – scheelite was different from the adsorption system of  $\text{H}_4\text{SiO}_4$  – calcite, or fluorite. Only one OH group of the  $\text{H}_4\text{SiO}_4$  molecule tilts toward the adjacent O atom, a H-bond was found between the hydrogen atom of  $\text{H}_4\text{SiO}_4$  molecule and the oxygen atom at the topmost layer of scheelite surface. The bond length of the new formed H-bond is 1.76 Å. The corresponding OH bond lengths of  $\text{H}_4\text{SiO}_4$  was stretched from 0.97 to 1.05 Å, which indicates a slight distortion of  $\text{H}_4\text{SiO}_4$  molecule during adsorption. The adsorption energy of a  $\text{H}_4\text{SiO}_4$  molecule on a scheelite (112) surface was -1.55 eV.

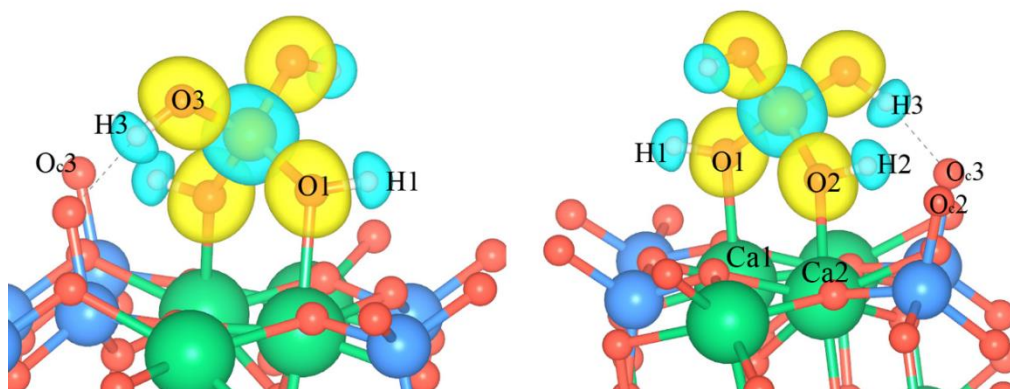


**Figure 8.** Charge density difference of the most stable adsorption configuration of a  $\text{H}_4\text{SiO}_4$  molecule on a scheelite (112) surface. An isosurface of charge density of  $0.003 \text{ e}/\text{Å}^3$  is employed, where charge depletion and accumulation were indicated in light greenish-blue and bright yellow, respectively. Color scheme: blue, green, yellow, red, and white represent W, Ca, Si, O and H atoms.

Bader charge of  $\text{H}_4\text{SiO}_4$  and scheelite surface was calculated to characterize the electron transport in the adsorption process. It can be seen that the scheelite (112) surface provides electrons to the  $\text{H}_4\text{SiO}_4$  molecule during adsorption. The charge density difference of the adsorption system was illustrated in Figure 8. The Oc3 atom bonding with H atoms of  $\text{H}_4\text{SiO}_4$  is found to be negatively charged, the negative charge decrease from  $1.45 e^-$  to  $1.41 e^-$ . The positive charge on the corresponding hydrogen atom decrease from  $0.67 e^-$  to  $0.63 e^-$ , whereas the negative charge on Oc3 atom increase by  $0.08 e^-$  and  $0.04 e^-$ . The significant increases in the O atom charge is contributed to the reduction of the electron density on the adjacent calcium atoms, and the Bader charges on the Ca1 and Ca2 atoms increased by  $0.02$  and  $0.01 e^-$ .

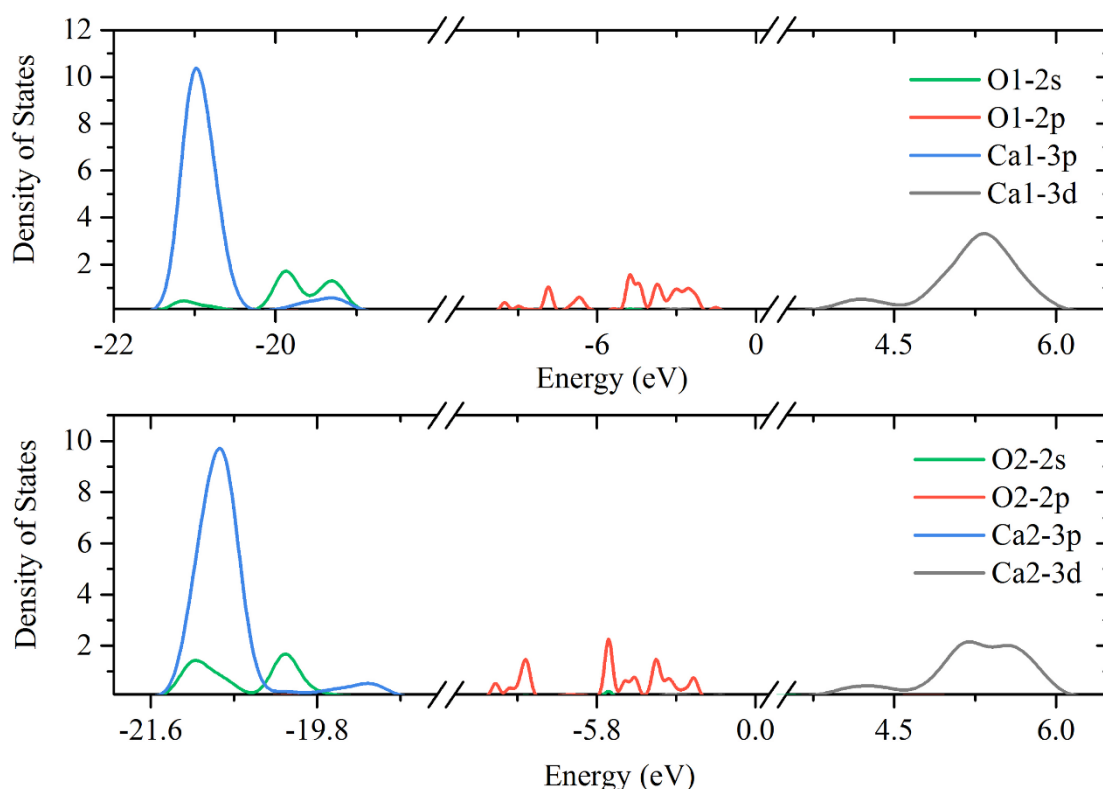


**Figure 9.** PDOS of the adsorption surface of the  $\text{H}_4\text{SiO}_4$ -scheelite (112) system. The calculated Fermi level is set as the zero point of x-axis. The curves correspond to the PDOS projected on to O atoms of  $\text{H}_4\text{SiO}_4$  molecule and the two adjacent Ca atoms. Ca1, and Ca2 are labeled in Figure 8.

The adsorption of  $\text{H}_4\text{SiO}_4$  molecule on scheelite surface leads a significant change of electronic structure; here we use PDOS analysis to characterize this change, which is plotted in Fig. 9.

The PDOS analysis results only showed that the electronic overlaps of the O-2s and Ca-3p orbital's in the adsorption system of  $\text{H}_4\text{SiO}_4$ -scheelite (112) surface, which was different with the adsorption of the  $\text{H}_4\text{SiO}_4$  molecule on the fluorite (111) or calcite (104) surface (including the overlaps of O-2p and Ca-3d). The overlaps caused the formation of Ca-O bonds between the O atoms of  $\text{H}_4\text{SiO}_4$  and Ca atoms of scheelite (112) surface.

Three characteristics of  $\text{H}_4\text{SiO}_4$  as a predominant hydrolysate of sodium silicate below pH 9.8 adsorbing on the surfaces of the three calcium minerals can be obtained:

- (i) Electrostatic interactions existed between the oxygen atom of  $\text{H}_4\text{SiO}_4$  molecule and calcium atom on the topmost layer of Ca-bearing minerals.
- (ii) Hydrogen bonds are found between the hydrogen atoms of the  $\text{H}_4\text{SiO}_4$  molecule and an oxygen atom or a fluorine atom of the Ca-bearing mineral surface.
- (iii) The OH groups in  $\text{H}_4\text{SiO}_4$  were significantly stretched during adsorption.

#### 4. CONCLUSIONS

$\text{H}_4\text{SiO}_4$ , a hydrolysate of sodium silicate, is the predominant species below pH 9.8 during adsorption in the flotation separation of calcium minerals. The adsorption of  $\text{H}_4\text{SiO}_4$  on calcite (104), fluorite (111), and scheelite (112) surfaces are probed in the present study by the employment of the DFT approach, with adsorption energies of -1.72 eV, -1.21 eV, and -1.55 eV, respectively. The results show that fluorite and calcite are the most and the least sensitive calcium mineral to the adsorption of  $\text{H}_4\text{SiO}_4$  during flotation separation, respectively. Molecular adsorption leads to the displacement of calcium atoms. Electrostatic interactions are found between the oxygen atom of  $\text{H}_4\text{SiO}_4$  molecule and the calcium on the topmost layer of Ca-bearing minerals. At the atomic level, the overlap between Ca-3p and O-2s orbital as well as Ca-3d and O-2p orbital is responsible for the formation of two Ca-O bonds when  $\text{H}_4\text{SiO}_4$  molecule are adsorbing on the surface of three kinds of Ca-bearing minerals.

The calculations also show that the OH groups of the  $\text{H}_4\text{SiO}_4$  can be only adsorbed on Ca-bearing mineral surfaces (labeled calcite (104), fluorite (111), and scheelite (112)) in molecular form, creating two hydrogen bonds between hydrogen atoms of  $\text{H}_4\text{SiO}_4$  and fluorine atoms of fluorite, two hydrogen bonds between hydrogen atoms of  $\text{H}_4\text{SiO}_4$  and oxygen atoms of calcite, and only one hydrogen bond between a hydrogen atom of  $\text{H}_4\text{SiO}_4$  and an oxygen atom of scheelite, respectively. Furthermore, the OH groups in  $\text{H}_4\text{SiO}_4$  are significantly stretched during adsorption. We believe that the results in this study may provide a fundamental insight for Ca-bearing mineral flotation.

#### ACKNOWLEDGMENT

Sponsored by K.C.Wong Magna Fund in Ningbo University.

#### CONFLICTS OF INTEREST

The authors declare no conflict of interest.

#### References

1. B. Feng, W. Guo, J. X. Peng, W. P. Zhang, *Purif. Technol.*, 199 (2018) 346.
2. N. R. Chevalier, *RSC Adv.*, 7 (2017) 45335.
3. F. Yang, W. Sun, Y. H. Hu, S. S. Long, *Miner. Eng.*, 81 (2018) 18.
4. W. P. Yan, C. Liu, G. H. Ai, Q. M. Feng, W. C. Zhang, *Int. J. Miner. Process.*, 169 (2017) 106.
5. R. D. Deng, Y. Q. Huang, Y. Hu, J. G. Ku, W. R. Zuo, W. Z. Yin, *Appl. Surf. Sci.*, 439 (2018) 139.
6. W. Chen, Q. M. Feng, G. F. Zhang, Q. Yang, *Miner. Eng.*, 126 (2018) 116.

7. H. L. Zhu, W. Q. Qin, C. Chen, L. Y. Chai, F. Jiao, W. H. Jia, *Miner. Eng.*, 120 (2018) 80.
8. W. Chen, Q. M. Feng, G. F. Zhang, Q. Yang, C. Zhang, *Miner. Eng.*, 113 (2017) 1.
9. C. Liu, Q. M. Feng, G. F. Zhang, W. Chen, Y. F. Chen, *Int. J. Miner. Process*, 157 (2016) 210.
10. Y. H. Hu, Z. Y. Gao, W. Sun, X. W. Liu, *Colloid Surface A*, 415 (2012) 439.
11. L. O. Filippov, A. Duverger, I. V. Filippova, H. Kasaini, J. Thiry, *Miner. Eng.*, 36-38 (2012) 314.
12. I. V. Filippova, L. O. Filippov, A. Duverger, V. V. Severov, *Miner. Eng.*, 66-68 (2014) 135.
13. X. Y. Wang, W. G. Liu, H. Duan, B. Y. Wang, C. Han, D. Z. Wei, *Powder Technol.*, 329 (2018) 158.
14. N. Wei, Luo, D. Z. Shen, Y. B. Liu, W. G. Gao, S. L. J. *Mater. Res. Technol.*, 7 (2018) 96.
15. Z. Y. Gao, D. Bai, W. Sun, X. F. Cao, Y. H. Hu, *Miner. Eng.*, 72 (2015) 23.
16. Chen, W. Feng, Q. M. Zhang, G. F. Yang, Q. Zhang, C. Xu, F. P. *Int. J. Miner. Process*, 169 (2017) 53.
17. M. A. M. Abdalla, H. Q. Peng, H. A. Younus, D. Wu, L. Abusin, H. Shao, *Colloid Surface A*, 548 (2018) 108.
18. Y. Zhang, Y. H. Wang, S. L. Li, *Int. J. Min. Sci. Technol.*, 22 (2012) 285.
19. M. C. Fuerstenau, G. Jameson, R. H. Yoon, Publisher: Society for Mining Metallurgy, and Exploration, Inc. Colorado, USA, 2007, pp: 502-511 ISBN-13: 978-0-87335-280-2.
20. B. Feng, X. P. Luo, J. Q. Wang, P. C. Wang, *Miner. Eng.*, 80 (2015) 45.
21. L. Y. Dong, F. Jiao, W. Q. Qin, H. L. Zhu, W. H. Jia, *Appl. Surf. Sci.*, 444 (2018) 747.
22. B. Li, S. Y. Liu, J. Y. Guo, L. Zhang, *Appl. Surf. Sci.*, 456 (2018) 215.
23. U. Aschauer, A. Selloni, *Phys. Rev. Lett.*, 106 (2011) 1.
24. J. Chen, F. F. Min, L. Y. Liu, C. F. Liu, F. Q. Lu, *Appl. Surf. Sci.*, 419 (2017) 241.
25. J. Liu, S. M. Wen, J. S. Deng, X. M. Chen, Q. C. Feng, *Appl. Surf. Sci.*, 311 (2014) 258.
26. Y. H. Han, W. L. Liu, J. H. Chen, *Appl. Surf. Sci.*, 370 (2016) 403.
27. Q. C. Feng, S. M. Wen, J. S. Deng, W. J. Zhao, *Appl. Surf. Sci.*, 396 (2017) 920.
28. A. Sarvaramini, F. Larachi, *Comp. Mater. Sci.*, 132 (2017) 137.
29. S. S. Rath, N. Sinha, H. Sahoo, B. Das, B. K. Mishra, *Appl. Surf. Sci.*, 295 (2014) 115.
30. M. Ernzerhof, G. E. Scuseria, *J. Chem. Phys.*, 110 (1999) 5029.
31. D. J. Chadi, *Phys. Rev. B*, 16 (1977) 1746.
32. E. Ataman, M. P. Andersson, M. Ceccato, N. Bovet, S. L. S. Stipp, *J. Phys. Chem. C*, 120 (2016) 16586.
33. R. M. Hazen, R. T. Downs, A. P. Jones, L. Kah, *Mineral. Geochem.*, 75 (2013) 7.
34. W. Jiang, Z. Y. Gao, W. Sun, J. D. Gao, Y. H. Hu, *Minerals*, 7 (2017) 1.
35. S. Speziale, S. T. Duffy, *Phys. Chem. Miner.*, 29(2002) 465.
36. Z. Y. Gao, W. Sun, Y. H. Hu, X. W. Liu, *Trans. Nonferrous Met. Soc. China*, 23 (2013) 2147.
37. M. I. Kay, B. C. Frazer, I. Almodovar, *J. Chem. Phys.*, 40 (1964) 504.
38. Y. Zhang, Y. Y. Li, R. Chen, Y. H. Wang, J. S. Deng, X. M. Luo, *Minerals*, 7 (2017) 1.
39. L. L. Hench, E. D. Clark, *J. Non-Cryst. Solids*, 28 (1978) 83.